#187 Dupl PUB-74-169-E FERMILAB-PUB-74-169-E #187 Phys. Rev. Letters

Heavy Particle Production in 300 GeV/c Proton/Tungsten Collisions

J.A. APPEL, M.H. BOURQUIN†, I. GAINES, L.M. LEDERMAN,
H.P. PAAR, J.-P. REPELLIN‡, D.H. SAXON, J.K. YOH
Columbia University, New York, N.Y.*
B.C. BROWN, J.-M. GAILLARD‡
National Accelerator Laboratory, Batavia, Illinois♀

---

* Research supported by the National Science Foundation, Washington, D.C.

† Swiss National Science Foundation Fellow.

‡ Visitors from Accélérateur Linéaire, Orsay, France.

♀ Operated by Universities Research Association, Inc. under contract with the U.S. Atomic Energy Commission.

ABSTRACT

A search was made for massive particles produced by 300 GeV/c protons. A 1.1 km flight path through a beam transport system permitted the measurement of the production of heavy particles for secondary momenta of 25 to 200 GeV/c. No counts were obtained for masses greater than 2 GeV/c^2 among 5.5×10^7 secondary particles. Cross sections are presented for forward production of π^+, π^-, p, $\bar{p}$, d, $\bar{d}$.

An experiment has been performed to measure the yields of heavy metastable particles produced by 300 GeV/c protons at the National Accelerator Laboratory (NAL). Results are given for π^+, π^-, p, $\bar{p}$, d, $\bar{d}$ rates and upper limits are set for the production of heavier objects.

Speculations concerning the existence of stable, massive particles outside of the known baryons and their anti-particles have largely been confined to the lowest mass in unitary symmetry triplets.[1] However, the possibility surely exists that there are entirely new families of objects analagous to leptons and baryons with stable ground state particles. If these have masses > 2 GeV/c^2, they could easily have escaped detection in the searches at older accelerators and in the cosmic rays. The high luminosity and energy of the NAL accelerator imposes an obligation to continue these explorations.

The principle of this observation consists of recording the time delay over a 1.1 km flight path (relative to pions of $\beta \simeq 1$) for particles of well defined momentum. The time delay method is greatly facilitated by the remarkably tight bunching in time of protons extracted from the NAL accelerator when the rf is left on during the extraction period. The rf structure peaks have a full width half maximum (FWHM) of 1.0 ns and are spaced 18.83 ns apart. This time coherence persists in the low mass secondaries during the 3 μs flight

path from the target. Heavier particles arrive after the $\beta = 1$ bunch. The time of flight difference is:

$$\Delta t = Lm^2(2cp^2)^{-1}$$

where L is the flight path, c the velocity of light, m the secondary particle mass and p the secondary momentum.

The mass range fixed by each momentum and the accessible delay times correspond to production "at rest" in the c.m., the most probable configuration for production of all known particles.

The measurements were made in the "Proton Center" beam line at NAL. The 300 GeV/c extracted proton beam of 5×10^{11} particles/pulse struck a tungsten target, ($\simeq$ 20% interaction length) placed 550 m from the main ring. The second part of the beam line, 1100 m long, was tuned to accept secondary particles of selected momenta produced at 0° by the primary interaction. The entire beam line was in vacuum to minimize secondary sources, multiple scattering, etc. It was composed of elements that normally transported the extracted beam to the Proton Center Laboratory, i.e., two vertical bends, one horizontal bend, two quadrupole doublets and steering magnets. The momentum bite was $\Delta p/p = \pm 1.4\%$ and the angular acceptance was $\Delta\Omega = 7 \times 10^{-9}$ sr. The apparatus is shown schematically in Fig. 1. The heavy particle signature was:

i) A triple coincidence in the counters $X_1 \cdot X_2 \cdot X_3 \equiv X$;

ii) No count in the counter C, a 7 m long air Cerenkov counter, normally at atmospheric pressure. This pressure permits the vetoing of pions at all momenta but will not veto the passage of particles of m/p such that $\Delta t \geq 0.9$ ns.

iii) No count in the counters P, a ring of four counters around the beam pipe. These three conditions made the event trigger ($X\bar{C}\bar{P}$).

iv) An anomalous time of flight from the target to the counters, X.

Four Δt's were recorded for each event. The particle was not timed near the target because of the large flux of locally produced particles. A reference timing signal was derived from the main accelerator 53.1 MHz rf oscillator, shaped in a fast trigger and prescaled by a factor 4 to a 13.3 MHz frequency. This was used as the stop signal to three Time-to-Amplitude Converters which used, respectively, X_1, X_2, X_3, gated by $X\bar{C}\bar{P}$, as the start signals. Pions provided four prompt ($\beta \simeq 1$) peaks in each Δt spectrum. The last Δt was measured from an intermediate counter (Y) to X_2. Comparison of this time to the others served to veto candidates for heavy particles produced by any failure of the rf bunching as happened in two pulses during the experiment. The counter Y (3 mm thick scintillator) was removed during 25 GeV/c running because it introduced unacceptable multiple scattering.

In the analysis, the Δt's were corrected (0.3 ns maximum) for the pulse height in the X counters. A weighted average of the three X-timings was made. Only two X-timings were used if the third differed by more than 1.0 ns from the average of the other two. The event was rejected if this was the case for all counters, if any X counter had a pulse height greater than three times minimum, or if both X_2 and X_3 had pulse heights above twice minimum. These cuts removed less than 15% of the data and did not affect any peak identification. Comparison with runs having an $X\bar{C}P$ trigger showed that no subtraction was needed for P-veto inefficiency. All of these corrections served to eliminate tails on the $\beta \simeq 1$ peaks due to local interactions of $\beta \simeq 1$ particles. The difference in time, X_1-X_2, had a FWHM of 0.85 ns, i.e., less than the bunch width, indicating that the rf bunch width was limiting the resolution. Typical Δt spectra are shown in Fig. 2, for negative particles at 24.5, 34.2, and 150 GeV/c, and positive particles at 50 GeV/c. The separation of the π^- and $\bar{p}$ peaks is further improved in runs with an $X\bar{P}$ trigger (not shown) on a scatter plot of time-of-flight difference against Cerenkov pulse height.

We find that the $\bar{p}/\pi^-$ ratios are within a factor 2 of the ones predicted by Grote et al[2] for an H_2 target. The measured cross sections for π^- and (π^+ + p) are given in Table I. They are lower than the thermodynamic model

predictions by a factor 2 to 4. The errors given include an uncertainty of the spot size on the target and errors in magnet and counter alignment. The experimental numbers are quoted assuming $\sigma_{TOT}(pW) = 1295$ mb. The 24.5 GeV/c peak at -10.5 ns (26 events) corresponds to antideuteron production nearly at rest in the c.m. Antideuterons and antiprotons were also observed at 34.2 GeV/c. Deuterons were observed at 25, 40 and 50 GeV/c. These results are summarized in Table II. The corrections for pion decay in flight were made to the pion cross sections and their ratios. At 40 and 50 GeV/c, π^+ and p are not separated and the d/π^+ ratios were calculated on the assumption that the π^+ greatly outnumber the p.[2]

K mesons and hyperons can be ignored as only a negligible fraction survive the flight path.

The fraction of antideuterons can be compared with the measurement of Binon et al[3] for 70 GeV/c p-Al collisions. At $x \equiv 2P_{||}/\sqrt{s} = 0.4$ in the c.m., they find

$$\bar{d}/\pi^- = (6.0 \pm 1.5) \times 10^{-7} .$$

For 30 GeV/c, p-Be collisions at 4 1/2° and x = -0.18,[4]

$$\bar{d}/\pi^- = (6.0 \pm 3.0) \times 10^{-8} .$$

These data suggest that the $\bar{d}$ cross section is rising with incident energy.

The $\bar{d}$ rate observed in this experiment is of the same order as that predicted by the model of Dorfan et al,[4] in

which two antinucleons are produced independently and overlap sometimes to make an antideuteron. They obtain a relation:

$$\left(\frac{\bar{d}}{d}\right) \simeq \left(\frac{\bar{p}}{p}\right)^2 ,$$

the $(\bar{p}/p)$ ratios being computed at half the outgoing deuteron momentum. Using the predictions of Grote et al[2] for $\bar{p}/p$, one obtains $\bar{d}/\pi^- \simeq 2 \times 10^{-5}$ at both momenta, in reasonable agreement with our data. Recent observations of $\bar{d}$ at 90° in pp collisions at the ISR[5] are not accounted for in this model. An interesting scaling exists for the ratio $(\bar{d}/\pi^-)[\bar{p}/\pi^-]^{-2}$ for all $\bar{d}$ observations.[5] One obtains: ISR: 5×10^{-3}; NAL: 8×10^{-3}; Serpukhov: 5×10^{-3} and BNL: 1.5×10^{-3}.

Not one trigger survived the analysis outside the Δt peaks due to known particles. The cross section limits for various outgoing momenta and heavy masses are shown in Table I. The intensity limits are 90% confidence levels, based on no events seen in 5.5×10^7 counts in total. The cross sections and ratios quoted are for the laboratory cross section $\partial^3\sigma/\partial p\partial^2\Omega$. The mass ranges are computed from the time of flight spectra beginning 0.5 ns (1/2 FWHM) from the last occupied bin. Mass ranges are quoted only for the interval

$$0 < \Delta t < 18.83 \text{ ns}.$$

Since times are measured modulo 18.83 ns, the limits also apply at higher mass ranges. The reader may calculate

these ranges using the formula:

$$m_n = (m^2 + 2cp^2 n\tau L^{-1})^{1/2}$$

for n = 1,2,3..., where τ = 18.83 ns and m,c,p,L are defined above, up to the kinematic limit.

A search was also made at -24.5, -34.2, +40, +50 (GeV/c/unit charge), for multiply charged particles, by demanding, in analysis, a pulse height greater than 3 times minimum in X_1, X_2 and X_3. Eleven candidates survived. They were identified by time of flight as follows: $4\bar{p}$, $2\pi^-$, 1p, $4\pi^+$. The upper limits in Table I therefore apply also to double-charged particles of twice the momentum. Production of ${}_2He^3$, ${}_2He^4$ and their antiparticles was not observed at these upper limits.

We wish to acknowledge the support of the National Accelerator Laboratory Proton Section and Accelerator Division, in particular Drs. J. Sauer and H. Edwards for their assistance in the rf structure studies. We also wish to thank Messrs. David Hom and David Snyder; Drs. P. Limon, E.T. Nash, and T. Yamanouchi for assistance and cheerful encouragement.

REFERENCES

1 F. Gursey, T.D. Lee, M. Nauenberg, Phys. Rev. 135, B467 (1964); H. Bacry, J. Nuyts, L. Van Hove, Phys. Letters 9, 279 (1964); Y. Hara, Phys. Rev. 134, B701 (1964); J. Schwinger, Phys. Rev. Letters 12, 237 (1964).

2 H. Grote, R. Hagedorn, J. Ranft. Atlas of Particle Production Spectra (CERN, 1970).

3 F. Binon et al, Phys. Letters 30B, 510 (1969).

4 D.E. Dorfan et al, Phys. Rev. Letters 14, 1002 (1965).

5 B. Alper et al, Phys. Letters 46B, 265 (1973).

TABLE I

Upper limits on forward production cross section of heavy particles for p-W collisions at 300 GeV for singly charged particles. (a)

Momentum (GeV/c)	x_π	$\frac{\partial^3\sigma_o}{\partial p\partial\Omega}$ (c) (mb/GeV/c/sr) per nucleon	Upper limit σ/σ_o (c)	Upper limit $\frac{\partial^3\sigma}{\partial p\partial\Omega}$ (μb/GeV/c/sr) per nucleon	Mass range (b) (GeV/c^2)
-24.5	0.08	1300	3.6×10^{-7}	0.39	1.22 - 1.67 1.97 - 2.31
-34.2	0.11	900	4.3×10^{-7}	0.33	1.54 - 1.59 2.14 - 3.28
-75	0.24	370	2.7×10^{-7}	0.10	3.1 - 7.0
-150	0.48	110	2.2×10^{-7}	0.024	5.6 - 13.9
-200	0.64	24	6.8×10^{-7}	0.016	7.5 - 18.7
+40	0.13	720	6.1×10^{-6}	4.4	2.18 - 3.73
+50	0.16	750	4.7×10^{-7}	0.35	2.46 - 4.64
+75	0.24	1330	7.5×10^{-8}	0.10	3.2 - 7.2
+150	0.48	1250	3.2×10^{-7}	0.40	5.5 - 14.1

(a) All cross sections have a systematic uncertainty ± 35%.
(b) Upper limits are also valid at higher masses (see text).
(c) σ_o is the measured π^- cross section for negative particles and the measured $(\pi^+ + p)$ cross section for positive particles.

TABLE II

Particle Production Ratios

momentum (GeV/c)	24.5	34.2	40	50
particle				
$\bar{d}$	26 $(4\pm1)\times10^{-6}$	39 $(11\pm2)\times10^{-6}$	-	-
$\bar{p}$	2436 $(2.0\pm0.1)\times10^{-2}$	1231 $(4.0\pm0.2)\times10^{-2}$	-	-
d	7 $(9\pm3)\times10^{-5}$	-	34 $(1.0\pm0.2)\times10^{-4}$	520±80 $(1.0\pm0.2)\times10^{-4}$
p	1562 $(9.0\pm0.3)\times10^{-2}$	-	-	-

Upper entry: Number of Events

Lower entry: Ratio to π's of same sign.

FIGURE CAPTIONS

Fig. 1 Schematic diagram of the apparatus

Fig. 2 Time-of-flight difference spectra for particles of unit charge and momentum -24.5, -34.2, -150 and +50 GeV/c. All events with $X\bar{C}\bar{P}$ trigger. The complete range is 18.83 ns; there are no counts outside the area shown.

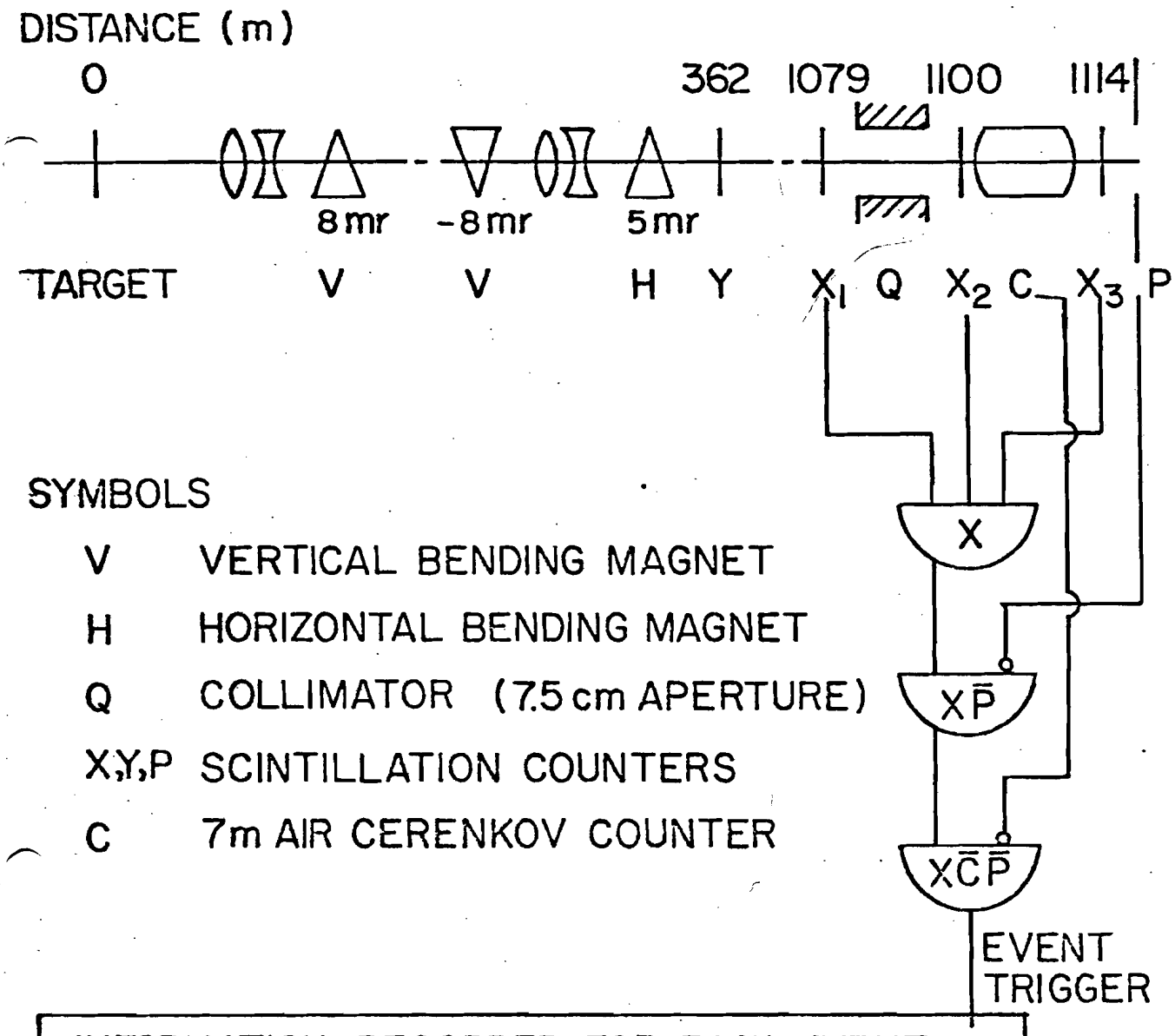

SYMBOLS

V	VERTICAL BENDING MAGNET
H	HORIZONTAL BENDING MAGNET
Q	COLLIMATOR (7.5 cm APERTURE)
X,Y,P	SCINTILLATION COUNTERS
C	7m AIR CERENKOV COUNTER

INFORMATION RECORDED FOR EACH EVENT

TIME 1	START X_1	STOP	13.3 MHz
TIME 2	START X_2	STOP	13.3 MHz
TIME 3	START X_3	STOP	13.3 MHz
TIME 4	START X_2	STOP	Y

PULSE HEIGHTS X1, X2, X3, C, Y

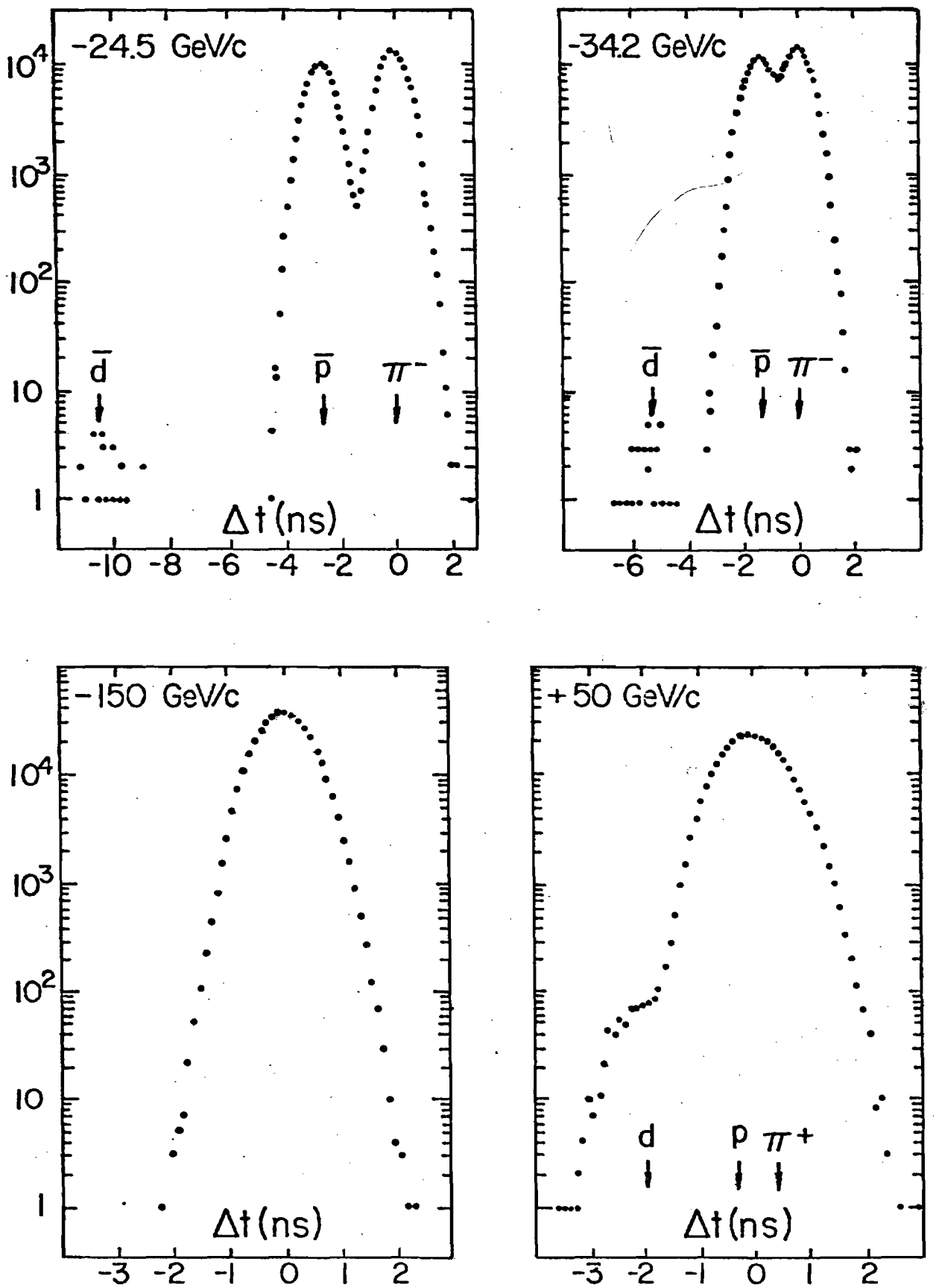
-24.5 GeV/c
10^4
10^3
10^2
10
1
$\bar{d}$
$\bar{p}$
π^-
Δt (ns)
-10 -8 -6 -4 -2 0 2
-34.2 GeV/c
$\bar{d}$
$\bar{p}$
π^-
Δt (ns)
-6 -4 -2 0 2
-150 GeV/c
10^4
10^3
10^2
10
1
Δt (ns)
-3 -2 -1 0 1 2
+50 GeV/c
d
p
π^+
Δt (ns)
-3 -2 -1 0 1 2